SSCL-479

SSCL-479

Superconducting Super Collider Laboratory

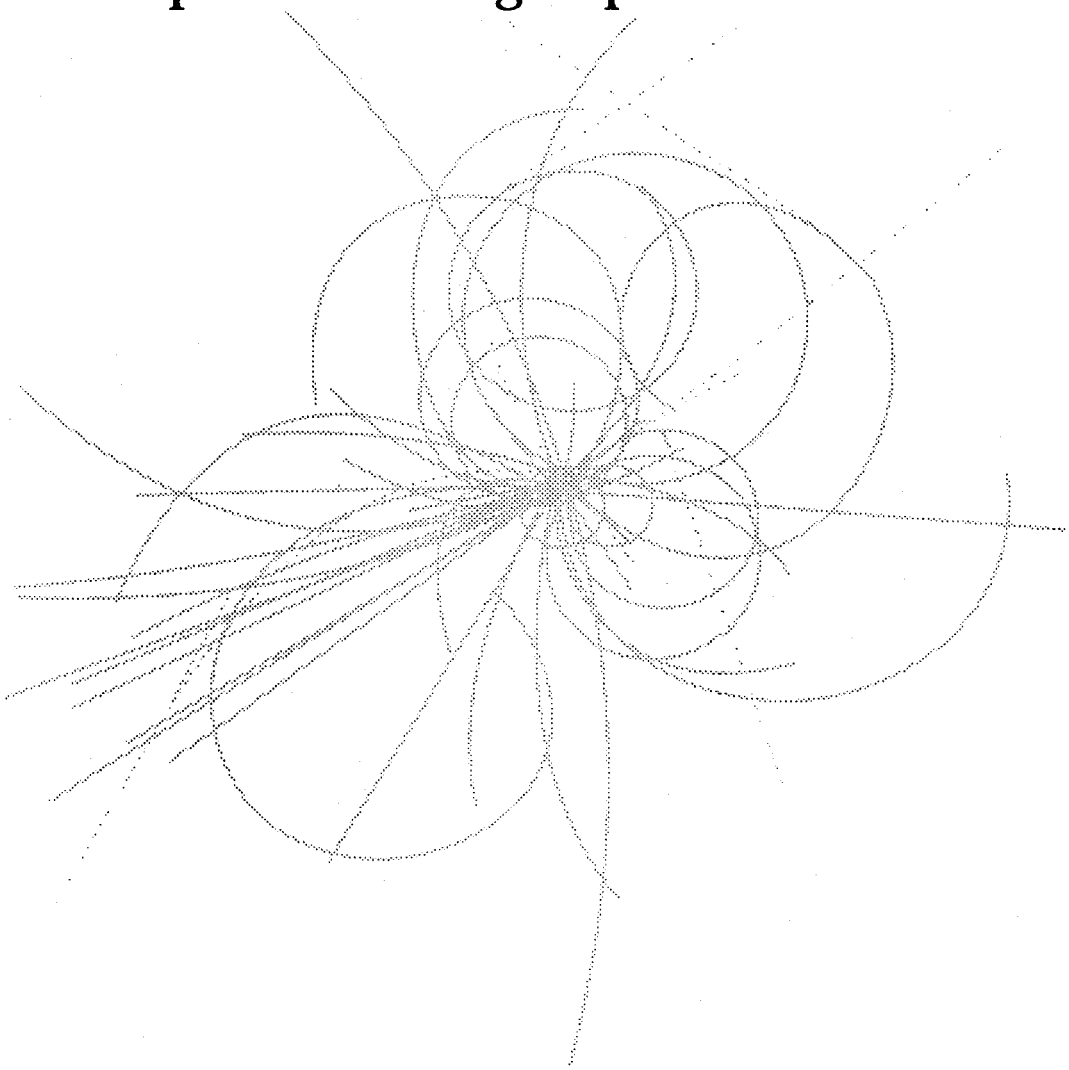

Supercomputing Activities at the SSC Laboratory

Y. Yan and G. Bourianoff

September 1991

SSCL-479

Supercomputing Activities at the SSC Laboratory*

Y. Yan and G. Bourianoff

Superconducting Super Collider Laboratory†
2550 Beckleymeade Avenue
Dallas, TX 75237

September 1991

* Invited talks presented at the DOE Energy Research Power Supercomputer Users Symposium, Gaithersburg, Maryland, May 21–22, 1991.

† Operated by the Universities Research Association, Inc., for the U.S. Department of Energy under Contract No. DE-AC35-89ER40486.

SSCL-479

Supercomputing Activities at the SSC Laboratory

Y. Yan and G. Bourianoff

Abstract

Supercomputers are used to simulate and track particle motion around the collider rings and the associated energy boosters of the Superconducting Super Collider (SSC). These numerical studies will aid in determining the best design for the SSC.

CONTENTS

SECTION I

1.0 INTRODUCTION 1
2.0 THE SSC LABORATORY 1
3.0 THE SUPER COLLIDER 3
4.0 SSC APERTURE STUDY 4
5.0 ORBIT DISTORTION EFFECTS 6
6.0 HEB APERTURE STUDY 7
7.0 SUMMARY AND FUTURE SUPERCOMPUTING NEED FOR THE SSC 8
ACKNOWLEDGEMENTS 10

SECTION II

1.0 INTRODUCTION 11
2.0 SPACE CHARGE EFFECTS IN THE LEB 12
3.0 DESIGN OF SIDE COUPLED CAVITIES IN THE LINAC 15

SECTION I
THE COLLIDER AND THE HIGH-ENERGY BOOSTER

by Y. Yan

1.0 INTRODUCTION

The Superconducting Super Collider (SSC) is a technologically advanced, high-energy physics research facility. Its construction and operation will ensure that progress continues in the search for answers to some of the basic questions about natural phenomena. The SSC will enable the study of fundamental particle interactions at energies ten times higher than those now available, in an energy region in which significant new phenomena are expected. The basic design goals for initial operation are to collide beams of oppositely-directed protons, with each beam at 20-TeV energy.

Besides the main collider itself—which consists of two vertically separated rings, each a 20-TeV accelerator with a circumference of 87 km—the SSC complex includes a cascade of energy booster accelerators (see Figure I-1). Each accelerator provides to the protons a successively higher energy before they enter the next accelerator. Protons are initially brought to 0.6 GeV in a linear accelerator. They then enter each of three booster synchrotrons: the low energy booster (LEB), which accelerates to 11 GeV in a 0.54-km circumference ring of magnets; the medium energy booster (MEB), which accelerates to 200 GeV in a 3.96-km ring; and the high energy booster (HEB), which accelerates to 2 TeV (2000 GeV) in a 10.9-km ring.

The initial design luminosity of $10^{33}\,\mathrm{cm}^{-2}\mathrm{s}^{-1}$ is obtained with 17,424 circulating bunches spaced 5 m apart, each with an intensity of about 10^{10} protons. The LEB and MEB use conventional magnets, while the HEB and collider ring use superconducting magnets. Beams cross from one collider ring to the other at four interaction points on the circulating beam orbits. Detector apparatus may be arrayed at each of the interaction points in order to conduct high-energy physics research experiments. In the future, alternate magnet strings will be provided to direct the proton beams around the detectors. The bypass will permit the collider to operate with beam in one leg of the bypass while detectors are constructed or serviced in the other leg.

2.0 THE SSC LABORATORY

In January 1987, after extensive project review of the SSC, the U.S. Department of Energy (DOE) and the Reagan Administration supported the project and recommended it to Congress. DOE initiated the process of site selection by issuing an Invitation for

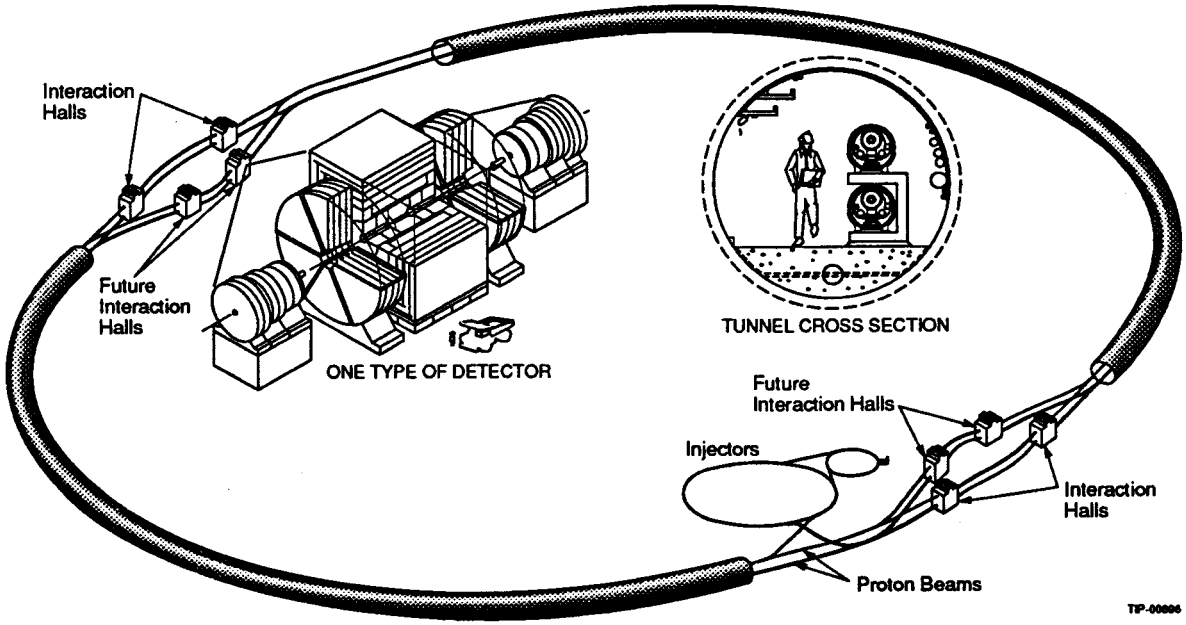

Figure I-1. A Schematic Layout of the SSC. The squares indicate the initial interaction regions. The dotted lines indicate future beam bypasses, which would make possible up to four additional interaction regions.

Site Proposals (ISP) in the spring of 1987. States submitted more than 40 site proposals to DOE. A special committee assembled by the National Academies of Science and Engineering recommended to DOE a select group of "best qualified sites." From this list, DOE chose the Texas proposal, with a site encircling Waxahachie, about 48.28 km south of Dallas (Figure I-2).

Concurrently with the extensive site selection efforts, DOE sought the services of a contractor to manage the design, and construction of the SSC, and the research program at the SSC Laboratory. It was announced in January 1989 that Universities Research Association (URA), in partnership with EG&G Intertech and Sverdrup Corporation, had been selected. URA announced the selection of Prof. Roy Schwitters of Harvard University as the director of the emerging SSC Laboratory. The first members of the new laboratory began work in the Dallas area in March 1989. By the end of the summer, more than 300 persons were working on the accelerator design, and component development, and were helping the launch of the new organization. There are now more than 1200 employees at the SSC Laboratory.

The SSC Laboratory will provide a full range of research capability for experimenters and theorists from around the world. Construction and utilization of a scientific instrument

of the scope of the SSC is a supremely challenging task. Its potential to advance basic knowledge and innovative technology is immense.

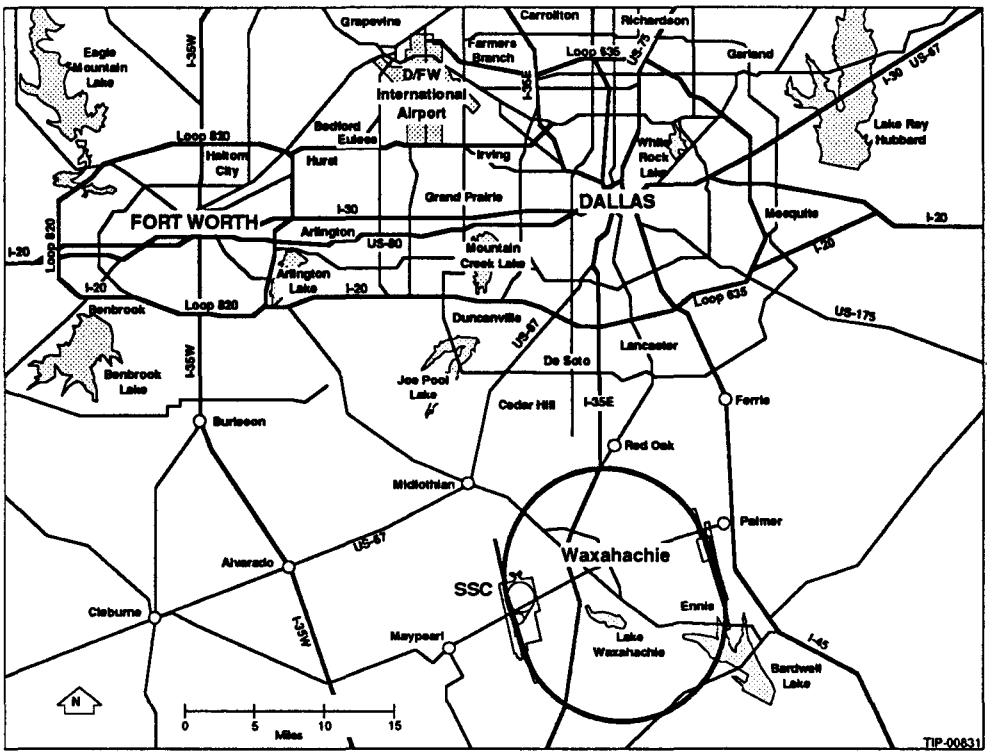

Figure I-2. Location of the SSC Site.

3.0 THE SUPER COLLIDER

The SSC will be a proton-proton collider with initial design luminosity of 10^{33} cm^{-2}s^{-1}. It will accelerate and guide bunches of ultra-high-energy protons into collision. Two tightly focused proton beams, each with an energy of 20 TeV, will move in opposite directions around a racetrack-shaped orbit. As the protons collide, their constituents can interact, thereby releasing enormous energy and revealing a level of detail that has never been achieved before. Direct evidence about the most fundamental physical forces and entities will be carried by the collision products and may be captured in the sophisticated detectors which will surround the interaction regions. Since the probability of interaction will be comparatively low, the proton beams can be recirculated to collide repetitively for many hours without significant attenuation. Thus the SSC will be constructed as a pair of storage rings capable of holding the tightly confined proton beams on closed paths for a day or more without replenishment. The rings confining the proton beams will be about 86.90 km in circumference and will be housed one above the other in an underground tunnel.

A system of superconducting electromagnets will guide the protons around the desired orbit through a beam pipe. This magnetic confinement system will consist of a periodic array of bending (dipole) and focusing (quadrupole) magnets, with the bending magnets establishing the curvature of the orbit and the focusing magnets confining the protons to a narrow region within the vacuum tube. The operating cycle of the SSC will begin with the collider magnets maintained at low current for about 40 minutes while the proton beams, with an energy of 2 TeV, are loaded into the collider rings from its high-energy booster. With injection complete, the acceleration system, powered with radio frequency (rf) waves, will be activated. The slow increase in the beam energy will be accompanied by a corresponding increase in the strength of the bending and focusing magnets, thus keeping the position of the beam orbit fixed while also keeping the proton beams synchronized with the accelerating system. This synchronous acceleration will be complete when the protons reach their final energy of 20 TeV. The accelerating system will then be turned down, and the beams will be steered into collision. The resulting reactions can be studied for a day or more before the beams are depleted to the extent that the cycle must be repeated. During the collision phase of the operation, some of the protons will be lost due to catastrophic nuclear collisions. In addition, the dynamics of the surviving beam particles will be perturbed by the electromagnetic interaction between the two beams at each collision point.

Success of the SSC operation will depend very much on the careful design of what is called the lattice, which is a detailed description of how the magnets of various types and strengths will be placed to form the confinement ring. The lattice encompasses both the physical arrangement and the powering or strength of the magnets. The most fundamental requirement for a good SSC lattice is that the proton beams have adequate lifetimes. Therefore, one has to understand the motion of the protons in detail so that suitable lattices for the SSC and its boosters can be designed. This requires extensive numerical studies. Supercomputers provided by the DOE supercomputer centers are very helpful in carrying out these required calculations efficiently.

In this paper, some of the typical numerical calculations for the SSC and the HEB, each of which requires a large amount of supercomputer time, are presented.

4.0 SSC APERTURE STUDY

One of the important issues for the SSC was the size of the superconducting dipole magnets to be used. More protons can survive in the collider rings with dipoles of larger coil diameter because larger coil-diameter dipole magnets can provide more uniform bending magnetic field. However, larger dipole magnets are more expensive. Therefore, one must

study the proton motion for each of the alternative magnet lattices under consideration. This was done by simulating the motion of the proton beam with numerical codes on supercomputers.

In these numerical studies, one starts with a well-designed linear lattice and then assigns systematic errors, random errors, and misalignment for the magnets, based on experience and measurement. Correction magnets may also be included. Ideally, protons are then tracked numerically for a limited number of turns to see if the motion is stable. At this stage, adjustment of the correction magnets is usually necessary (somewhat similar to the micro-tuning of a TV or a radio). After the accelerator is well tuned, one can start short-term tracking (say, 400 turns) to study some well-defined accelerator physics criteria to predict the behavior of the accelerator.

A typical short-term-tracking phase space plot is shown in Figure I-3. The variation in the amplitude traced out by given protons is greater for those protons of larger initial amplitude. Here, as shown in Figure I-3, the amplitude is defined as $\sqrt{x^2 + p_x^2}$, where x is a Floquet space coordinate and p_x is its corresponding Floquet space momentum; that is, they are normalized such that a proton with linear motion would trace out a circle in (x, px) phase space. This phenomenon serves as a diagnostic of accelerator nonlinearity. If the amplitude variation is considered too big for a certain desired amplitude, the corresponding accelerator design should be modified.

Generally, one would be more concerned with the long-term stability of the protons. One would like to track hundreds of protons (with appropriate initial amplitude distributions) around the ring element-by-element for 100,000 turns or more (0.5 minutes of SSC operation will be about 100,000 turns). Using a current scalar computer would require months of Central Processing Unit (CPU) time, since there are more than 10,000 magnet elements in the SSC machine. Fortunately, however, the protons in the beam may be considered to be independent from each other, so that a tracking code can be completely vectorized over the number of particles; thus, a supercomputer is ideal for this purpose. One can track many particles (say, 64 protons) simultaneously, saving enormous CPU time over what a scalar machine would require.

Figure I-4 compares the tracking data up to 100,000 turns for a collider injection lattice (at 2 TeV energy) using 4-cm coil-diameter dipole magnets with the corresponding data for the same lattice using 5-cm coil-diameter dipole magnets. None of the particles with initial displacement amplitude of less than 8.1 mm were lost in the 5-cm coil-diameter dipole magnet case; but in the 4-cm coil-diameter dipole magnet case, particles still get lost until their initial displacement amplitude is reduced to about 5.3 mm. The only difference

between the two lattices was in the multipole content, due to the different size of the magnet aperture. With the increase in magnet aperture from 4-cm coil-diameter to 5-cm coil-diameter, the stable region of the proton motion for 100,000 turns enlarged from about 5.3 mm to about 8.1 mm in radius. Based on these numerical studies and many other investigations, the 5-cm coil-diameter superconducting dipole magnets have been chosen.

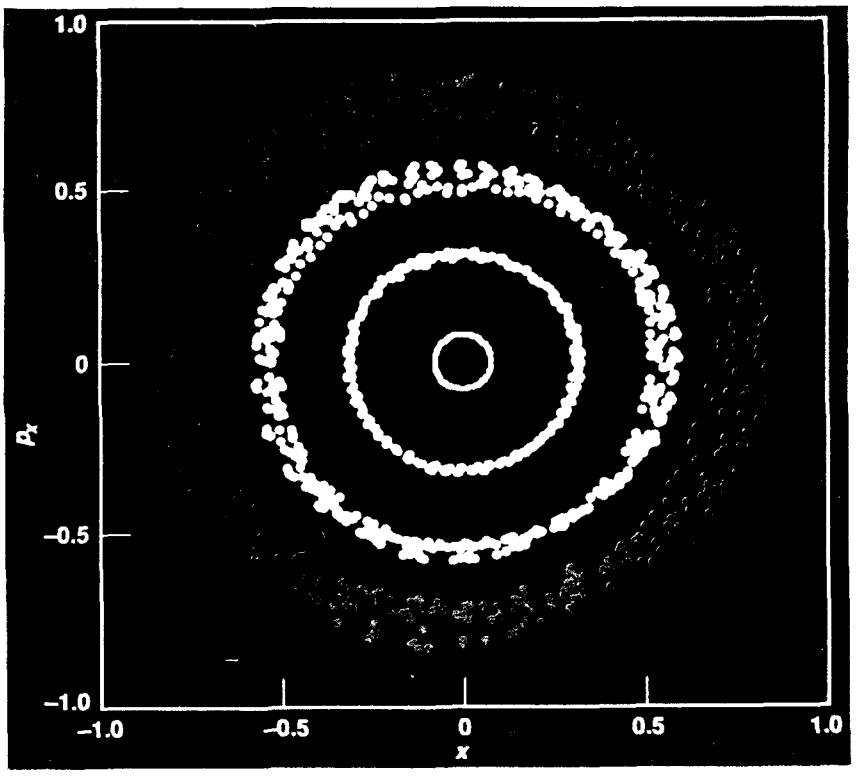

Figure I-3. Phase Space Plot p_x vs. x for Four Protons With Different Initial Amplitudes, Where x is a Floquet Space Coordinate and p_x is its Corresponding Floquet Space Momentum; that is, They are Normalized Such That a Proton With Linear Motion Would Trace out a Circle. The variation in the amplitude traced out by a given proton serves as a diagnostic of accelerator nonlinearity of that proton's motion. For example, the protons here with the smallest initial amplitude show so little nonlinearity that the data points merge into a solid line. However, the protons with the largest initial amplitude have correspondingly greater nonlinearity, so that the data points are more widely spaced in the circular band.

5.0 ORBIT DISTORTION EFFECTS

Alignment of the magnets along the rings may not be perfect. Therefore, correctors are needed to correct the proton orbit along the ring. As a guide for future commissioning, we have also carried out computer simulations on different orbit distortions. A typical result is shown in Figure I-5. The stable transverse region of the proton motion in the collider ring is reduced with a larger RMS orbit distortion. Although the stable region of the protons is much reduced with a 3-mm RMS orbit distortion, there is only slight reduction

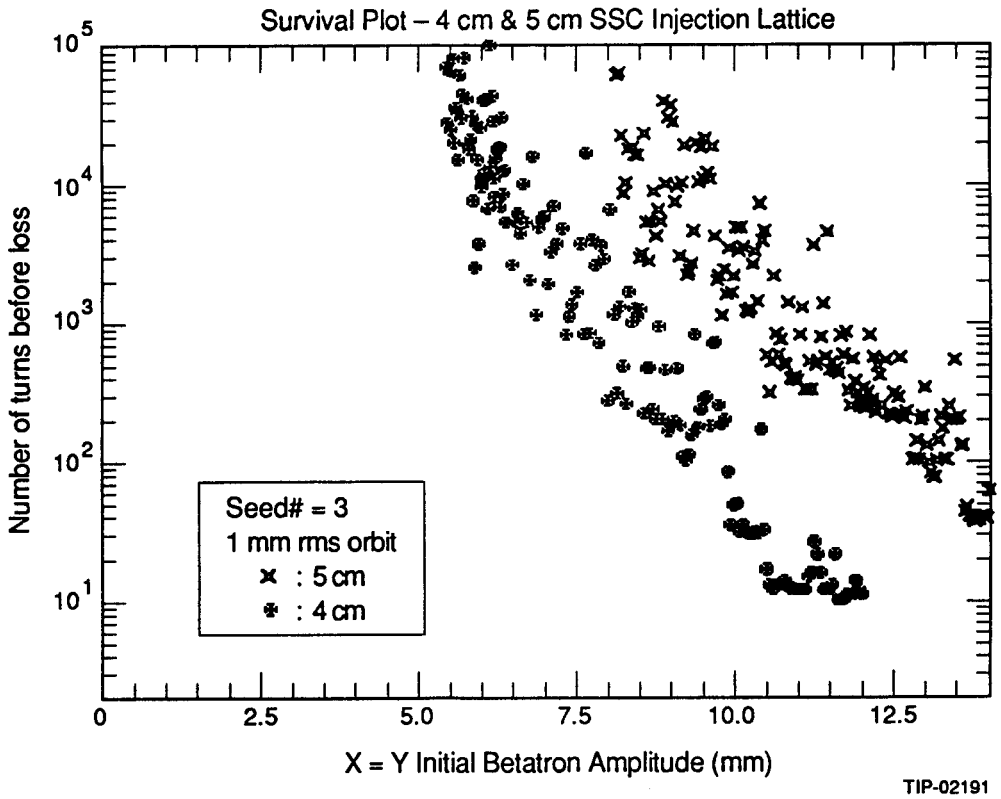

Figure I-4. A Hundred-Thousand-Turn Survival Plot for a Collider 2-TeV Injection Lattice, Comparing the Data for a 5-cm Magnet Aperture With the Data for a 4-cm Magnet Aperture. With the 5-cm aperture, no particles with initial displacement amplitude of less than 8.1 mm were lost. By increasing the magnet aperture, the dynamic aperture for 100,000 turns enlarges from about 5.3 mm to about 8.1 mm in radius, which increases the machine's linearity. (This plot shows only the protons that were lost before 100,000 turns are reached.)

for the transverse stable region from a 1-mm RMS orbit distortion to a 2-mm RMS orbit distortion.

6.0 HEB APERTURE STUDY

Successful SSC operation depends on the proper design not only of the collider itself but also of its associated energy boosters. Because both the collider and the HEB use superconducting magnets, the HEB aperture study—like the collider aperture study—requires much supercomputer time. Figure I-6 shows survival plots for a typical HEB aperture study. Each of Figure I-6(a) and Figure I-6(b) shows 5 sets of tracking data from 5 different random assignments of multipole errors from the same RMS error description. The differences between Figure I-6(a) and Figure I-6(b) are due to different RMS multipole errors, which are larger for the 5-cm coil-diameter dipole magnets than for the 7-cm coil-diameter dipole magnets. Although there are some differences in the transverse stable regions of the proton motion among different random error assignments of the same RMS

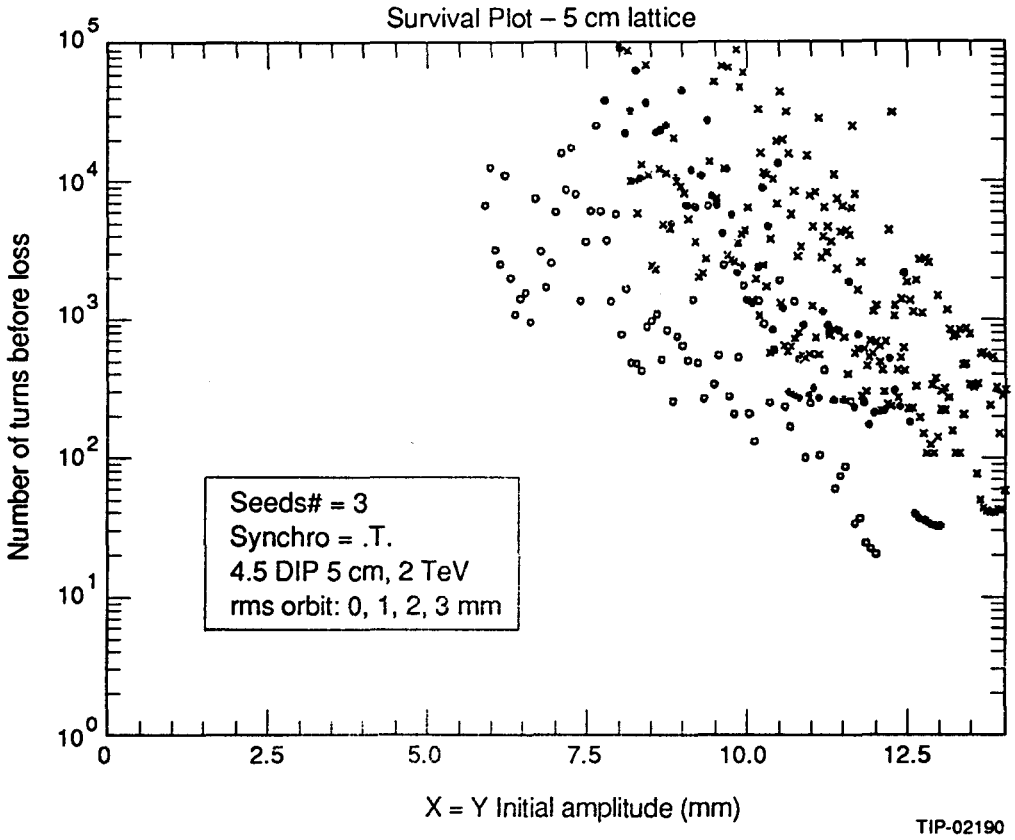

Figure I-5. A Hundred-Thousand-Turn Survival Plot for a Collider 2-TeV Injection Lattice, Comparing the Data for a 5-cm Magnet Aperture With 4 Sets of Different Orbit Distortions. The RMS orbit distortions are 0 mm, 1 mm, 2 mm, and 3 mm respectively. Larger orbit distortions result in smaller stable regions.

error, there is a larger difference in the transverse stable region between the two cases (a) and (b) using different sizes of dipoles. These and other studies as well as budget consideration have led to the selection of the 5-cm coil-diameter superconducting dipole magnets for the HEB.

7.0 SUMMARY AND FUTURE SUPERCOMPUTING NEED FOR THE SSC

Some typical numerical results for the study of the SSC involving use of the supercomputers provided by the DOE supercomputer centers are presented. There are many other supercomputing activities at the SSC Laboratory, including studies of magnet design, cryogenics, and detector. Calculations associated with the lower energy boosters (the Linac and the LEB), which have also required large amounts of resources, are discussed in a companion paper by George Bourianoff.

Each component of the SSC complex must be designed properly to ensure successful operation. Since all of these designs involve a high degree of nonlinearity in mathematical formulation, numerical calculations are required. Actually, large-scale computer simulations

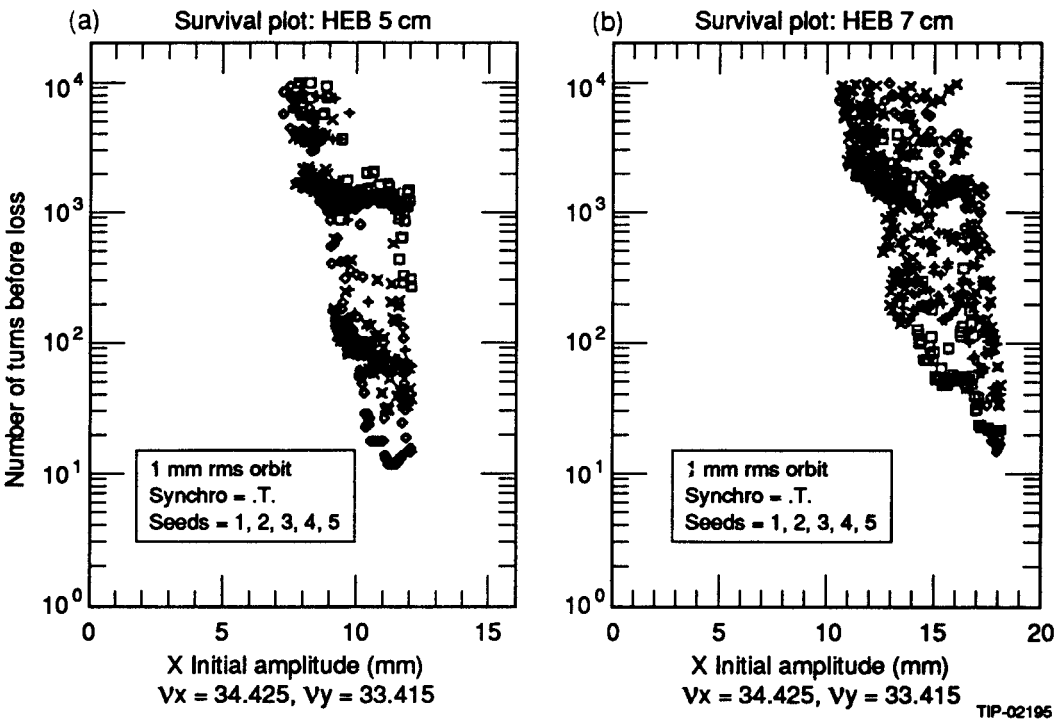

Figure I-6. 10,000 Turn Survival Plots for the HEB Aperture Study. Each set of the symbols represents the data for each of the 5 seeds.

are probably the only way to obtain a detailed understanding of each component of the SSC.

ACKNOWLEDGEMENTS

The work reported here was made possible by the cooperation of many colleagues at the SSC Laboratory. Among those the author wishes to acknowledge are G. Bourianoff, S. Dutt, D. Johnson, L. Schachinger, and T. Sen. In particular, the author wishes to thank A. Chao, the principal investigator for SSC supercomputing, for his continuing encouragement and support.

SECTION II
LOW ENERGY BOOSTER AND COUPLED CAVITY LINAC

by G. Bourianoff

1.0 INTRODUCTION

Since humans became curious about the world around them, they have sought answers to two basic questions: What are things made of? How do they work? The answers to these questions have evolved over time, affecting in deep and pervasive ways how we live and how we view the universe and humankind's place in it. In just the past two decades, spectacular progress using ever more powerful particle accelerators and more sensitive detectors has found new answers with remarkable insights into the evolution of the universe and the natural laws that govern the behavior of matter at all times and places.

However, some of the deepest questions can only be addressed by observing phenomena at energies that are significantly higher than today's accelerators can reach. So, several years ago, we began asking ourselves how best to explore, in a timely and thorough manner, the territory richest in clues to a more complete understanding of matter and energy.

The SSC Laboratory has been established to design, build, maintain and operate the Superconducting Super Collider, a high energy subatomic particle accelerator that will be used in basic research to learn more about the fundamental nature of matter and energy. When completed in 1999, the Super Collider will be the most powerful subatomic particle accelerator in the world. It will propel two beams of protons in opposite directions at velocities near the speed of light before colliding them in huge detector halls. There the debris from these collisions will be recorded so that scientists may study the results to learn more about the fundamental particles and forces of the universe. The energy of the proton collisions will be so great that it will recreate conditions that may have prevailed at the very moment of creation of the universe, the moment of the "Big Bang."

During the past year, the SSC has made significant use of the MFE computer center for simulating the low energy accelerators in the SSC complex. Simulation associated with the high energy superconducting accelerator have also required large amounts of resources, but they are discussed in a companion paper by Yiton Yan. The work reported in this paper was done by others with the author merely serving as a reporter. The people most responsible for the actual work are: S. Machida, and Chu-Rui Chang.

There are two primary supercomputer applications reported. They are the calculation of emittance growth in the LEB due to space charge effects and simulation of the side coupled cavities used in the linac.

2.0 SPACE CHARGE EFFECTS IN THE LEB

The SSC is designed to have a luminosity of 10^{33} interactions per second per square centimeter. It directly determines the amount of physics which can be done with the collider and is therefore of critical importance. The luminosity is inversely proportional to the emittance of the two colliding beams. Since emittance increases monotonically through the chain of accelerators, an emittance budget has been set up defining what the allowable emittance increase is in each individual component of the accelerator. The emittance budget for the LEB calls for the emittance to enter the LEB at 0.4π mm-mrad and leave the LEB at 0.6π mm-mrad. Therefore, a set of simulations was done to determine the actual emittance growth.

The simulation was done with TEAPOT, a general purpose accelerator tracking code modified to include space charge effects. The space charge module computes the transverse electrostatic forces on a given particle created by the other particles. The primary effect of the space charge is to produce an electric field which increases linearly with radius and will therefore produce the same effect as a quadrupole magnet, i.e., a tune shift. The tune shift for a Gaussian beam is given by Eq. (1).

$$\Delta\nu = \left(-\frac{r_p}{4\pi}\right) \frac{N_B M}{\beta\gamma^2\, \epsilon_N\, B_f}\,. \tag{1}$$

Since $\Delta\nu$ is inversely proportional to $\beta\gamma^2$, the tune spread is largest where $\beta\gamma^2$ is smallest, i.e., the LEB. In addition to the tune shift, there is a tune spread produced by non-uniform beam distribution. The effect of tune spread is to bring the beam into contact with resonances it would not normally encounter as shown in Figure II-1.

The figure shows the region of tune space occupied by the beam as well as primary resonance lines in the accelerator. The operating point of the LEB was taken to be 11.85 and 11.80 and the total tune shift $\Delta\nu$ is 0.6. Therefore, the effect of tune shift is to spread the beam across the 1/2 and 1/3 integer resonances which are well-known to produce emittance growth. The study consisted of a thorough investigation of the LEB lattice in an attempt to find an optimal solution. The study included varying the operating tune, several difference lattice arrangements, two injection energies and a sensitivity analysis to different levels of multipole fields.

The principle result is shown in Figure II-2. It shows the emittance growth for 600 MEV injection energy. The figure shows that after 8000 turns the emittance has almost stopped increasing and the goal of 0.6π mm-mrad is approximately met.

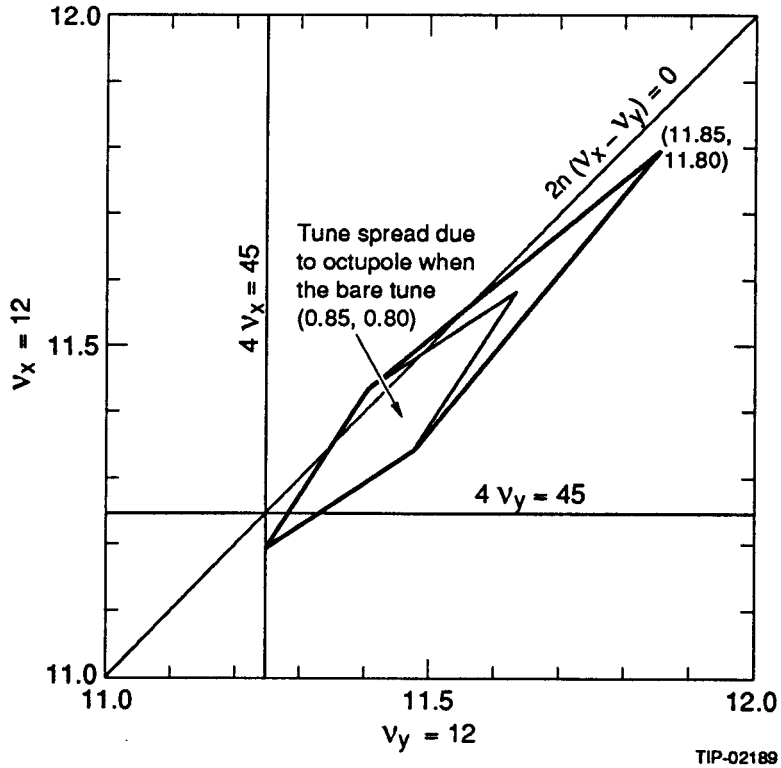

Figure II-1. Tune Space Operation of the LEB.

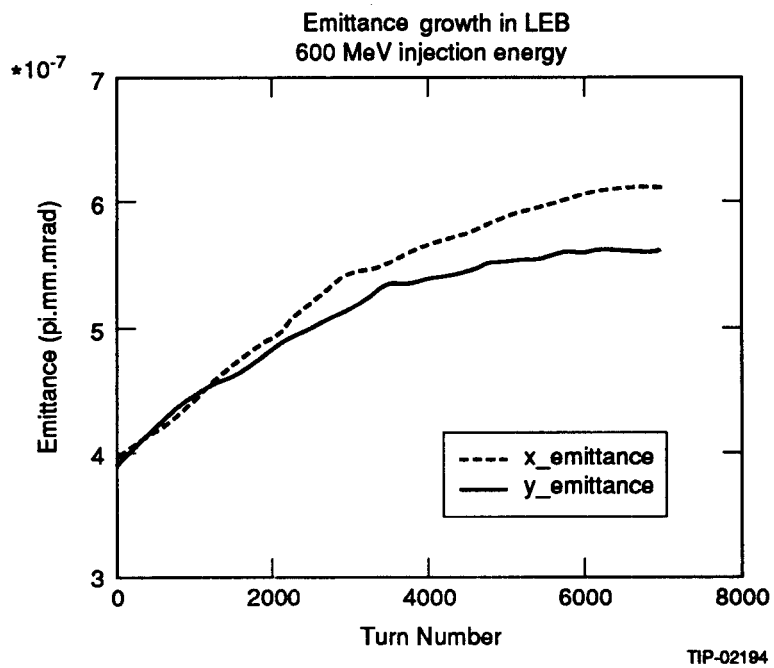

Figure II-2. Emittance Growth in LEB as a Function of Turn Number.

The calculation shown in Figure II-2 required about 30 hours of CPU time on the Cray 2. The addition of the space charge calculation increases the running time of the code by a factor of 10 relative to the same calculation without space charge. The reason for this dramatic increase is that the space charge calculation imposes a numerical stability requirement of the frequency of calculation which would not otherwise exist. The result is that the space charge calculation has to be performed every $5\,ns$ of the cycle whereas the calculation associated with magnetic elements is performed every $50\,ns$. The entire study described here required approximately 300 hours of machine time.

A final part of this study was to calibrate the code against experimental data taken at Fermilab. The basic measured data gave the emittance as a function of beam intensity as shown by the squares in Figure II-3.

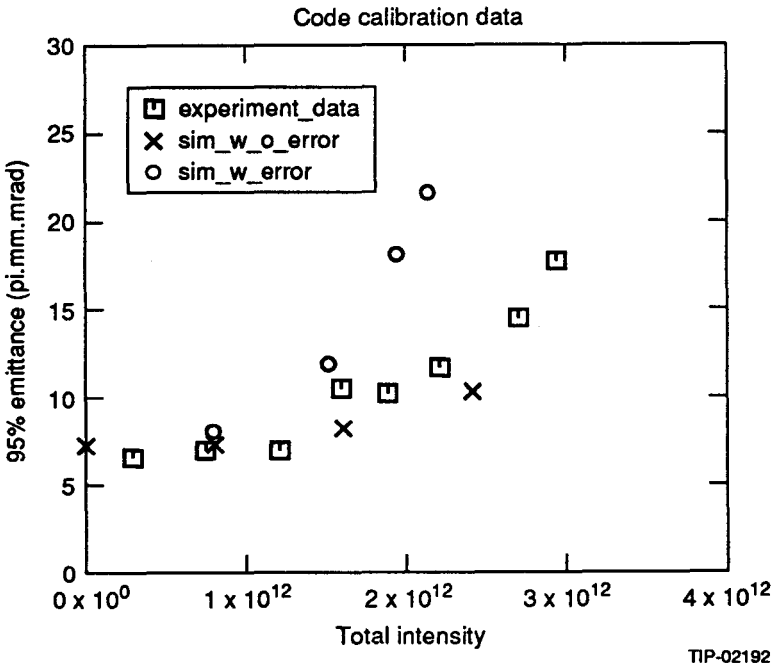

Figure II-3. Code Calibration Run.

The magnitude of magnetic multipole errors in the experiment was not known so the simulation was done for two cases, one in which the errors were zero and one containing a worst case estimate of the errors indicated respectively by the circles and dots in Figure II-3. It can be seen that the simulation results bracket the experimental results thereby providing a convincing check of the code accuracy. It can be seen that the code even reproduces the knee in the curve at 1.25×10^{12}.

3.0 DESIGN OF SIDE COUPLED CAVITIES IN THE LINAC

The linac is designed to accelerate 25 mA of H^- ions from 70 MEV to 600 MEV. There are several possible cavity designs which might be used but the side coupled cavity design operating in the $\pi/2$ mode has a number of advantages concerning operating stability and ease of manufacture. It has therefore been chosen for the linac accelerator.

Figure II-4 shows the conceptual layout of one module consisting of 6 tanks powered by one 20 MW klystron.

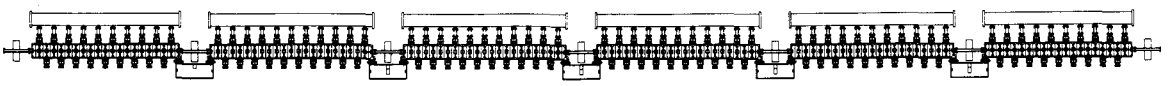

Figure II-4. Schematic Diagram of One CCL Module.

Each module has 6 tanks that is coupled by 5 bridge couplers. A detail of one accelerating cavity is shown in Figure II-5. It can be seen that the coupled cavity linac is inherently a three-dimensional object. However, it can be shown that the coupling slots in the accelerating cavities make only a small change in the accelerating cavity fields and hence a majority of the design work can be done with SUPERFISH. The coupling cavity design work, however, must use MAFIA-3D. The three-dimensional nature of the simulation requires use of 3 hours of Cray time-per-design run on 450,000 mesh points.

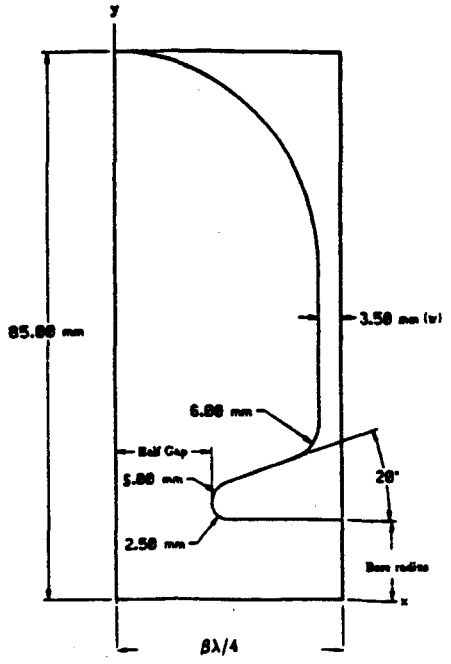

Figure II-5. Geometry of an Accelerating Cavity.

A critical parameter for the accelerating cavity is the shunt impedance, defined to be ratio of the square of the accelerating field to the power dissipated. The shunt impedance is determined by the cavity geometry, especially the cavity radius and the dimensions of the nose cone. After a systematic study, the cavity radius was chosen to be 8.5 cm and the curvatures R_{n1}, R_{n2}, and R_{n3} were chosen to be 0.6 cm, 0.5 cm and 0.25 cm respectively. The electric fields associated with the TM010 mode are shown in Figure II-6.

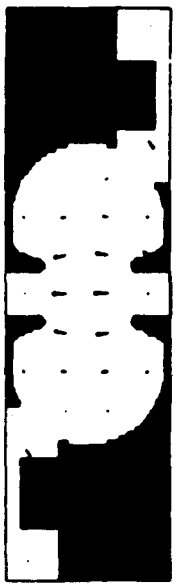

Figure II-6. Electric Fields in an Accelerating Cavity.

The length of the accelerating cavity must be $\beta\lambda/2$ to efficiently accelerate the particles. Therefore, the length of each cavity changes to compensate for the change in β down the accelerator.

Each module contains 5 quadrupoles to maintain the focus down the linac. The electromagnetic energy must be coupled around the quadrupoles by bridge couplers. The bridge couplers in the CCL vary in length from $5/2\lambda$ on the low energy side to $3/2\lambda$ on the high energy side. The longer bridge couplers ($5/2\lambda$) tend to have problems with mode mixing, unless they are carefully designed. Mode mixing excites frequencies other than the desired frequency in the bridges and this leads to additional dissipation. The unwanted modes can be suppressed by inserting resonant posts at strategic locations or by using conducting rings to separate the long bridges into a multicavity resonator. The later method seems to do a better job of discriminating against unwanted modes. Figure II-7 shows a MAFIA plot of a multicavity bridge along with end tank accelerating cavities and coupling cavities. The simulations that generated this plot are some of the most demanding that have ever

been done for this type of problem requiring 400,000 mesh points and 3 hours of Cray time-per-run.

The final phase of CCL design is to check the beam dynamics through the modules. The strength of the focusing quads was determined with the program TRACE 3D. The beam envelope equations were then integrated through the linac using the program CCLDYN. Figure II-8 shows the energy spread, phase spread and x envelope spread as a function of energy. The predicted emittance at the end of the linac is 0.271π mm-mrad. This will feed into the LEB and meet the LEB input requirement of 0.4π mm-mrad.

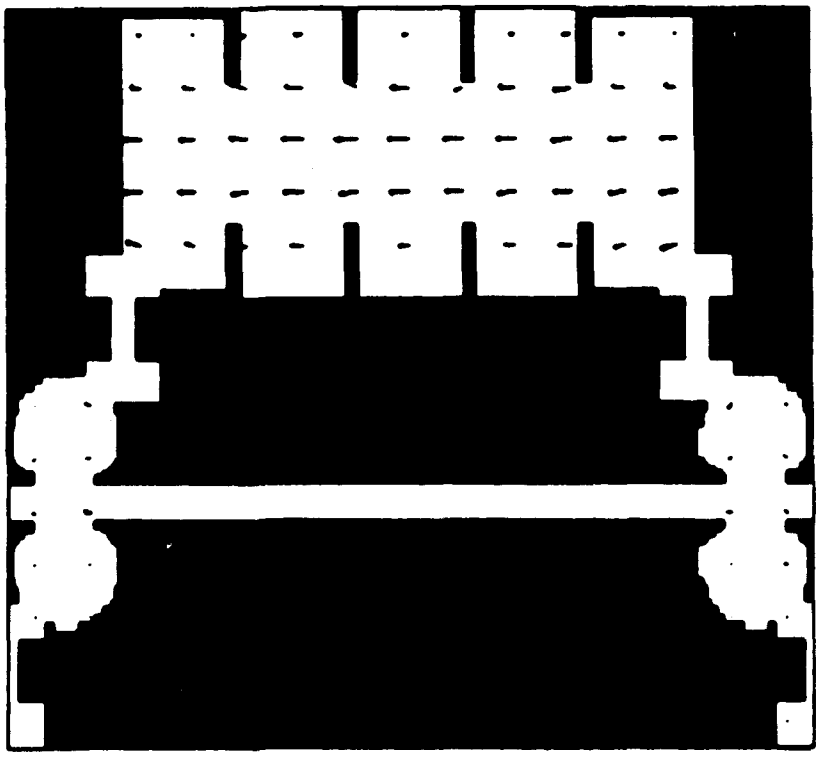

Figure II-7. Electric Fields in Bridge Coupler.

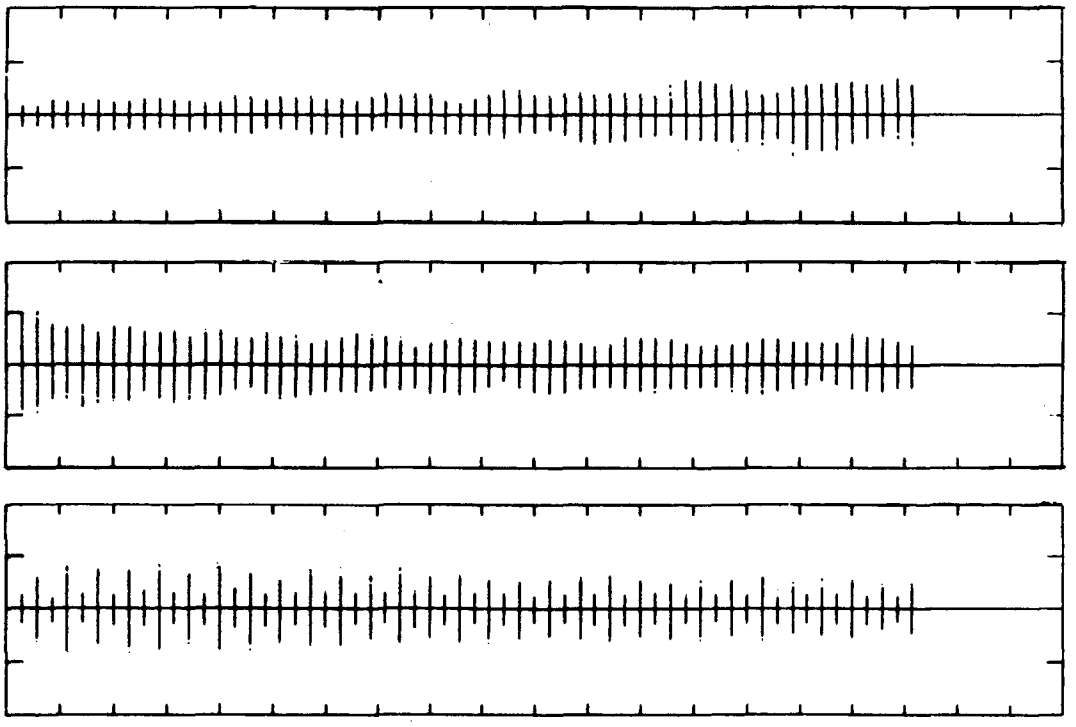

Figure II-8. Beam Energy, Phase and Size Down the Linac.